Published in final edited form as:
Acta Biomater. 2013 May ; 9(5): 6576–6584. doi:10.1016/j.actbio.2013.02.006.

Semi-Interpenetrating Network (sIPN) Gelatin Nanofiber Scaffolds for Oral Mucosal Drug Delivery

Donald C. Aduba Jr.[1], **Jeremy A. Hammer**[2], **Quan Yuan**[1], **W. Andrew Yeudall**[3,4], **Gary L. Bowlin**[1], and **Hu Yang**[1,4,*]

[1]Department of Biomedical Engineering, Virginia Commonwealth University, Richmond, VA 23284

[2]Departments of Pharmaceutics and Pharmaceutical Chemistry, Bioengineering & Utah Center for Nanomedicine, University of Utah, Salt Lake City, UT 84112

[3]Philips Institute of Oral and Craniofacial Molecular Biology, Virginia Commonwealth University, Richmond, VA 23298

[4]Massey Cancer Center, Virginia Commonwealth University, Richmond, VA 23298

Abstract

The oral mucosa is a promising absorption site for drug administration because it is permeable, highly vascularized and allows for ease of administration. Nanofiber scaffolds for local or systemic drug delivery through the oral mucosa, however, have not been fully explored. In this work, we fabricated electrospun gelatin nanofiber scaffolds for oral mucosal drug delivery. To improve structural stability of the electrospun gelatin scaffolds and allow non-invasive incorporation of therapeutics into the scaffold, we employed photo-reactive polyethylene glycol diacrylate (PEG-DA575, 575 $gmol^{-1}$) as a cross-linker to stabilize the scaffold by forming semi-interpenetrating network gelatin nanofiber scaffolds (sIPN NSs), during which cross-linker concentration was varied (1X, 2X, 4X, and 8X). The results showed that electrospun gelatin nanofiber scaffolds after being cross-linked with PEG-DA575 (i.e., sIPN NS1X, 2X, 4X, and 8X) retained fiber morphology and possessed improved structural stability. A series of structural parameters and properties of the cross-linked electrospun gelatin scaffolds were systematically characterized in terms of morphology, fiber diameter, mechanical properties, porosity, swelling and degradation. Mucin absorption onto sIPN NS4X was also confirmed, indicating this scaffold possessed greatest mucoadhesion properties among those tested. Slow release of nystatin, an anti-fungal reagent, from the sIPN gelatin nanofiber scaffold was demonstrated.

Keywords

drug delivery; electrospinning; nanofiber; tissue engineering; buccal mucosa

*Address correspondence to: Hu Yang, Department of Biomedical Engineering, Virginia Commonwealth University, 401 West Main Street, Richmond, P.O. Box 843067, VA 23284, hyang2@vcu.edu, Tel: (804) 828-5459, Fax: (804) 828-4454.

Disclosure Statement

No competing financial interests exist.

1. Introduction

Oral mucosa as a drug absorption site possesses many characteristics with advantages such as high accessibility, ease of self-administration, high blood supply for drug circulation, avoidance of first-pass effect and reduction of systemic and allergic side effects [1, 2]. Various oral mucosa drug delivery vehicles in different dosage forms have been developed including solutions, tablets (lyophilized and bioadhesive), sprays, etc. Newer delivery systems in forms of chewing gum, laminated systems, patches, hydrogels, adhesive films and microspheres have been designed to provide sustained drug release into the oral mucosa after rapid onset [3–5]. General features expected of delivery systems for local drug delivery to the oral mucosa include biocompatibility, mucoadhesiveness, stability, non-immunogenicity, and capability of sustained drug release to maintain therapeutic levels over an extended period of time[6, 7]. It is not uncommon to utilize a combination of these dosage forms to maximize clinical efficacy. Meanwhile, patient compliance and adherence for a new dosage form should also be considered in developing local oral drug delivery formulations.

Oral candidiasis (oral thrush), a fungal infection of the oral mucosa, may benefit from new dosage form development. Symptoms of candidiasis include erythema or white patches in the mouth. Patients suffer pain, discomfort and loss of appetite [8, 9]. It commonly spreads to involve the esophagus, pharynx, and even to other areas of the body as a secondary infection [9]. Currently, formulations including tablets, mouth washes, and patches have been used to deliver therapeutics to treat oral candidiasis with success. However, the transient activity and systemic toxicity of those therapeutics taken orally can be problematic [4]. Thus, local oral mucosal drug delivery route could be a better approach to candidiasis treatment. Electrospun nanofibers have been actively studied in tissue engineering scaffolding over the last decade [10–12]. They have been explored for clinical applications in wound healing, orthopedics and cellular/tissue regeneration [13–15]. Electrospun scaffolds have nanoscale and microscale fiber architecture with a high surface to volume ratio and high porosity, enabling high drug loading and interaction with epithelial cells of the oral mucosa [16]. Therefore, nanofiber scaffolds can be a suitable platform for oral mucosal drug delivery. Nonetheless, utility of nanofiber scaffolds for oral candidiasis treatment has yet to be fully explored.

In this work, we fabricated gelatin nanofiber scaffolds via electrospinning and explore them for local delivery of therapeutics for candidiasis. The advantages of electrospun fibers for oral mucosal drug delivery are i) high surface area to volume ratios; ii) the ability to directly and locally adhere the scaffold onto the site of infection; and, iii) allowing tuning of the physical properties of the scaffold to control and optimize drug delivery at the infection site while maintaining its structural integrity during dosing. Gelatin nanofibers are beneficial due to their biocompatibility and mucoadhesive properties, allowing local and sustained release at the absorption site [17]. A noticeable problem with electrospun gelatin nanofibers is their low structural stability in aqueous phases. It is crucial to maintain nanofiber structural features and stability during application. To this end, we explored photocurable PEG diacrylate as cross-linker to stabilize gelatin nanofiber scaffolds by forming semi-interpenetrating network nanofiber scaffolds (sIPN NSs). Although PEG diacrylate (PEG-DA) has been used to form sIPNs with gelatin or other polymers in solution form [18, 19], the use of PEG-DA to form sIPNs with nanofibers has not been investigated. Different from short cross-linkers such as glutaraldehyde, 1-ethyl-3-(3-dimethylaminopropyl) carbodiimide hydrochloride (EDC), and genipin [20, 21] that would react directly with gelatin to form cross-linked gelatin networks, PEG-DA has a longer chain and undergoes free radical polymerization of terminal acrylates to form a PEG network without reaction with gelatin. Therefore, the use of PEG-DA would be expected to minimally affect nanofiber

morphology. The structure, nanofiber morphology, mechanical and physical properties of the resulting sIPN gelatin nanofiber scaffolds as well as effects of modulation of cross-linker concentration on their structural features and properties were investigated in this work. Delivery and release of nystatin, an anti-fungal drug commonly used for oral candidiasis treatment, from the sIPN gelatin nanofiber scaffold was studied.

2. Materials and Methods

2.1. Materials

Polyethylene glycol diacrylate (PEG-DA575, M_n =575 g/mol), sodium hydroxide, 2,2 dimethoxy-2-phenylacetophenone (DMPA), calcium chloride, and porcine type-A gelatin were purchased from Sigma-Aldrich (St. Louis, MO). 1,1,1,3,3,3-hexafluoro-2-propanol (HFP) was purchased from TCI America (Portland, OR). Ethanol (200 proof, KOPTEC) was purchased from DLI (King of Prussia, PA). Phosphate buffered saline (PBS) was purchased from EMD Chemicals (Gibbstown, NJ). Dulbecco's modification of eagle's medium (DMEM) was purchased from Invitrogen (Carlsbad, CA). Sodium chloride, nystatin and monopotassium phosphate were purchased from Fisher Scientific (Fair Lawn, NJ). Protein assay dye reagent concentrate was purchased from Bio-Rad (Hercules, CA). Mucin (gastric) was purchased from Pfaltz & Bauer (Waterbury, CT). Spectral/Por molecular porous regenerated cellulose dialysis tubing MWCO 12–14000 was purchased from Spectrum Laboratories (Rancho Dominguez, CA).

2.2. Scaffold preparation

As illustrated in Scheme 1, preparation of sIPN NSs involved two steps: electrospinning and cross-linking.

2.2.1. Preparation of electrospinning solutions—One gram of gelatin was added to 10 mL of HFP. The mixture was shaken continuously for 24 h to obtain a homogeneous transparent gelatin/HFP solution. To prepare drug loaded gelatin solutions, 1 g of nystatin was added to 10 mL of the gelatin/HFP solution. The mixture solution was vortexed vigorously to completely dissolve nystatin into a homogenous solution. The vial was placed on a shaker plate and shaken continuously for 24 h.

2.2.2. Preparation of gelatin nanofiber scaffolds (NSs)—To fabricate electrospun gelatin fibers, the gelatin solution was drawn up through the blunted needle (18G×1½ in) of a 10 ml syringe. The syringe was loaded into a syringe pump, propelling the gelatin solution out of the needle 125 mm away from the collecting mandrel at a rate of 5 ml/hr. The needle was connected to a positive electrode of a high voltage power supply (Spellman CZE100R, Spellman High Voltage Electronics Corporation). The positive electrode applied 25 kV voltages to the needle. This voltage created an electric field opposite to the grounded target to overcome the surface tension at the needle tip. These conditions generated a Taylor cone which allowed a steady stream of gelatin solution to flow from the needle to the grounded collecting plate in a jet-like fashion. As the gelatin solution was being streamed from the needle tip, the HFP solvent evaporated. Randomly aligned nanofibers were collected on a flat, stainless steel mandrel (7.5 cm×2.5 cm×0.5 cm, L× W×T) rotating at 500 rpm.

2.2.3. Preparation of sIPN gelatin nanofiber scaffolds (sIPN NSs)—Gelatin NSs were cross-linked with various doses of PEG-DA575 in the presence of DMPA to obtain sIPN NSs. 1X, 2X, 4X, and 8X cross-linker solutions were prepared by dissolving appropriate amounts of PEG-DA575 and DMPA in ethanol, in which 1X is defined as 56 mg/mL PEG-DA575 and 2 mg/mL DMPA. When concentration of PEG-DA575 was increased, concentration of DMPA was increased proportionally to maintain constant the

ratio of PEG-DA575 to DMPA. A defined volume of cross-linking solution (2 mL) was poured on an NS (7.5×2.5 cm×0.5 cm) and allowed to incubate for 30 min. The scaffold was held under UV light (UVP Blak-Ray Long Wave Lamp, 100 Watts) from a 14 cm distance for 2 min on each side of the scaffold and then air-dried.

For comparison, gelatin NSs were incubated with ethanol only for 30 min and air-dried to obtain NSEs. Conventional gelatin sIPN hydrogel scaffolds (sIPN HS4X) having the same composition as sIPN NS4X were also prepared. PEG-only hydrogel scaffolds (i.e., PEG-only HS) were also prepared by mixing 150 mg of PEG diol 1500 dissolved in 1 mL of deionized water, 1.12 g of PEG-DA575, and 4 mg of DMPA followed by 10-min UV exposure.

2.3. Scanning electron microscopy (SEM)

Prior to SEM imaging, scaffolds were placed on a 1 cm diameter stub. The stub was placed on a specimen holder and gold sputter coated. SEM images were taken on a Zeiss EVO 50 XVP Scanning Electron Microscope. Sixty randomly chosen fibers in each SEM image were analyzed with UTHSCSA ImageTool™ software for fiber diameter measurement.

2.4. Tensile testing

“Dog-bone” shaped samples (n=10) were obtained using a punch die (ODC Testing & Molds) of the dimensions 19.05, 3.175 and 6.1 mm at its length, narrowest point and widest point, respectively. Mechanical properties of the samples, including peak load, peak stress, modulus, strain at break and energy to break, were tested using the MTS Bionix 200 Mechanical Testing System in conjunction with TestWorks 4.0 software.

2.5. Porosity measurements

Gelatin nanofiber samples (1 cm×1 cm) (n=5) were cut out and weighed. The thickness was measured with a digital caliper. The apparent volume (V_a) of the scaffold was then determined. The volume of the material (V_g) was determined on the basis of densities of gelatin (1.41 g/cm^3) and PEG-DA575 (1.12 g/cm^3) and their mass percent compositions. The porosity was then calculated based on the following equation adapted from Hu et al. [22]:

$$Porosity = [1 - (V_g / V_a)] \times 100 \quad \text{(eq. 1)}$$

2.6. Swelling studies

Nanofiber samples (1 cm×1 cm) (n=5) were placed in wells filled with 5 mL of pH 7.4 PBS (one sample per well) at room temperature (24 °C). They were taken out at predetermined time intervals, immediately blot dried, weighed, and placed back in the solution. Swelling ratio (SR) was calculated using the following equation.

$$SR(\%) = (W_s - W_d) / W_d \times 100 \quad \text{(eq. 2)}$$

where W_s is the weight of the swollen sample, and W_d is the initial weight of the sample.

2.7 In vitro degradation studies

In vitro degradation of the fabricated scaffolds was evaluated in either DMEM supplemented with 10% fetal bovine serum (FBS) or simulated saliva fluid (SSF) (12 mM KH_2PO_4, 40 mM NaCl, 1.5 mM $CaCl_2$, with NaOH adjusted to pH 6.2 [23]) at 37 °C. Samples of 1 cm diameter (n=9) were weighed and individually immersed in a well filled

with 1.5 mL of one of the two media mentioned above. At 6 h, 12 h and 24 h, samples were taken out and centrifuged at 9.3×10^3 *g* for 20 min. After centrifugation, the residue was collected, freeze dried, and weighed. The amount of mass loss due to degradation was calculated according to the following equation:

$$ML(\%)=[(W_o-W_d)/W_o]\times 100 \quad \text{(eq. 3)}$$

where ML is mass loss due to degradation, W_o is the initial mass of the scaffold, and W_d is the mass of the residue after incubation for a given length of time and freeze drying.

2.8. Mucin absorption assay

Mucoadhesiveness of sIPN NS2X, 4X, and 8X (n=8) was indirectly tested by measuring absorption of mucin onto the scaffold. Each scaffold was immersed in 1 mg/mL mucin solution and taken out immediately. The concentration of mucin in the remaining solution was assessed spectrophotometrically by Bradford protein assay. Gelatin contamination was quantified by performing an additional set of studies, in which gelatin-containing scaffolds were immersed in a blank solution and immediately drawn out to determine the amount of gelatin eluted in to the medium. These values were then subtracted from the experimental values (scaffolds containing mucin) to calculate the correct amount of mucin absorbed. The amount of mucin absorbed onto the scaffold was then determined and normalized to surface area of the scaffold because direct interfacing between the scaffold and oral mucosa tissue is observed over surface area instead of surface volume. Mucin absorption on PEG-only HS and sIPN HS4X was measured for comparison.

2.9. Cell attachment assay

sIPN NS4X scaffold (n=3) was positioned on the bottom of a well in a 48-well tissue culture polystyrene (TCPS) plate. An O-ring was placed on the scaffold to prevent the scaffold from floating. 5000 human dermal fibroblasts were seeded on the scaffold and allowed to adhere and grow for 48h. To image adherent cells on the scaffold with SEM, the scaffold was gently washed with PBS, fixed by 2% glutaraldehyde in 0.1M cacodylate buffer, and kept refrigerated prior to imaging. To quantify cell attachment, another set of scaffolds were washed gently with PBS. The adherent cells were collected following trypsinization and counted with trypan blue assay.

2.10. Drug release studies

Release of nystatin from sIPN NS2X, 4X and 8X was studied because these scaffolds displayed relatively good structural stability in aqueous solutions. Nystatin-loaded scaffolds were immersed in pH 7.4 PBS and placed in dialysis tubing with molecular weight cut-off (MWCO) of 12000–14000 Da. At predetermined time points up to 120 h, a 1 mL aliquot was withdrawn from the release medium. One mL of fresh PBS, pre-equilibrated at 37 °C, was immediately added to maintain its volume. Absorbance of nystatin was measured at 305 nm as reported in literature [24]. The cumulative drug release was then reported. The amount of nystatin loaded in each sample was estimated after the release profile curve reached a plateau over time, indicating a complete release of the drug.

2.11. Statistical analysis

Statistical analysis was carried out using one way analysis of variance (ANOVA) and Holm-Sidak method for subgroup comparison. P values less than 0.05 were considered statistically significant.

3. Results and Discussion

3.1. Fiber morphology and diameter

Since gelatin is not soluble in ethanol, ethanol was used as a medium facilitating cross-linking of electrospun gelatin fibers. Although cross-linking treatment inevitably caused the electrospun scaffolds to lose definition due to fiber fusion within the network, the nanodomains and porous structure of the scaffold did not fully collapse, and fine fiber filaments were conserved (Figure 1). Interestingly noted is a pronounced fiber collapse found within NSE, a gelatin NS incubated in ethanol only.

Mean fiber diameter, an important characteristic of nanofiber scaffolds, was measured based on SEM images. Incubating gelatin nanofibers in ethanol alone caused a significant fiber diameter reduction. This was due, in large part, to the shrinking of hydrophilic gelatin fibers in an organic solvent. In particular, there was a 23% decrease in diameter of ethanol treated scaffolds as compared to uncross-linked nanofibers ($p<0.001$) (Figure 2). The mean fiber diameters of NSE, sIPN NS2X, and sIPN NS8X were similar to each other ($p>0.05$). Gelatin nanofibers treated with 2X or 4X cross-linker ethanol solution possessed the lowest mean fiber diameter. Although fiber diameter of nanofibers was affected by cross-linking and ethanol, regardless of cross-linker concentration, no significant morphological differences were observed among all the cross-linked scaffolds. The scaffolds from each individual treatment displayed fiber fusion and a well distributed porous structure. It is unclear why 8X cross-linker solution did not reduce fiber diameter of cross-linked electrospun gelatin scaffolds as significantly as 2X and 4X. We postulated that fiber diameter of cross-linked gelatin fibers is influenced by several other factors such as chain length, distribution of cross-linker, its interaction with gelatin fiber, elasticity of the cross-linked network, etc. Higher cross-linker concentrations tend to generate more densely cross-linked networks. Meanwhile, the formed network becomes less elastic. Therefore, fiber diameter reduction caused by cross-linking density increase resulting from application of 8X may have been compromised by the network becoming more rigid, preventing an appreciable structural change as found in gelatin fibers cross-linked with 2X or 4X PEG-DA575.

3.2. Tensile properties

Tensile testing was conducted to evaluate how gelatin nanofiber scaffolds mechanical properties were influenced when the PEG-DA575 cross-linker concentration was adjusted. The results are summarized in Table 1. Thickness, peak load, peak stress, modulus, strain at break and energy to break were all significantly higher in NSE samples as compared to NS samples. Scaffolds treated with increasing cross-linker concentration exhibited lower peak stress values from 17.48 MPa to 6.61 MPa as the concentration of PEG-DA575 was increased from 1X to 8X. Elastic modulus also declined cross-linker concentration increased. sIPN NS1X failed at 554.5 MPa, while sIPN NS8X failed at 155.5 MPa. sIPN NS4X and sIPN NS8X exhibited compromised elasticity. The modulus decreases with an increase in crosslinker concentration because higher crosslinked scaffolds have less of a tendency to deform elastically while returning to its original shape. By definition, elastic modulus quantifies the stress to strain ratio thus, sIPNs NS4X and NS8X exhibited the lowest modulus values because their crosslinking densities enabled the scaffold's length to change more easily from the original state, inducing higher strain values.

3.3. Porosity and swelling

As shown in Figure 3, NS and NSE exhibited an average porosity of 82% and 85%, respectively, and their difference in porosity was not statistically significant ($p>0.05$). Porosity of sIPN NS decreased as cross-linker concentration increased from 1X to 4X. The data was consistent with a previous report that increasing cross-linker concentration reduces

fiber diameter and porosity of the cross-linked electrospun scaffold [25]. Higher concentrations of PEG-DA575 increased cross-linking density and fiber interconnecting, leading to smaller diameters and lower porosity within the gelatin scaffold. sIPN NS4X had the lowest average porosity at 29%. Similarly, sIPN NS8X possessed a compromised porosity, which was comparable to that of sIPN NS2X.

Swelling kinetics of electrospun gelatin fibers receiving different treatments studied in pH 7.4 PBS at room temperature varied (Figure 4). Their swelling ratios following 24 h equilibration were dissected and compared. At 24 h, NS achieved highest swelling ratio, which was 824±46%. In contrast, swelling ratio of NSE was 529 ±20%, significantly lower than that of NS but comparable to that of sIPN NS1X. The degree of swelling among cross-linked samples was inversely dependent on cross-linker concentration. sIPN NS8X had the lowest swelling ratio at 24 h, which was five times lower than that of sIPN NS1X. The lower degrees of swelling in sIPN NS4X and 8X samples were due to the presence of a denser cross-linked network, limiting water absorption. In contrast, scaffolds cross-linked with less PEG-DA575 tend to have a greater proportion of pores within flexible nanofiber architectures to facilitate water absorption.

3.4. In vitro degradation

Uncross-linked gelatin nanofibers quickly liquefy and completely dissolve in aqueous solutions due to rapid phase transition from solid to solution at 37 °C [26, 27]. NS and NSE degraded completely in minutes post-immersion, and no solid residue was obtained using the method described in the degradation studies. This is presumably a reflection of incomplete cross-linking and the way sIPN NSs were prepared.

1X cross-linking was insufficient retaining the structural integrity either. Mass loss of sIPN NS1X in 6 h was close to 100% (Figure 5A). Nevertheless, mass loss due to degradation was significantly reduced with increasing cross-linker concentration. When cross-linker concentration was increased to 2X, the scaffold retained 11.0% of its mass on average in DMEM/10% FBS over a 24 hour period. sIPN NS4X and sIPN NS8X scaffolds retained 41.3% and 67.1% of its original mass on average in DMEM/10% FBS over 24 hours. This suggested that gelatin nanofibers became increasingly stable in aqueous solutions as cross-linker concentration was increased. A similar trend was also observed in SSF. However, impact of incubation period on scaffold degradation was negligible in contrast to the impact of cross-linking concentration although sIPN NS2X lost less mass after a 24-h incubation in SSF as compared to its degradation with 6-h and 12-h incubation within the same media.

Furthermore, the cross-linked scaffolds became less stable in SSF than in DME/10% FBS (Figure 5B). For example, sIPN NS8X retained 41.1% of original mass on average in solid, which was only 60% of the remaining scaffold residue in DME/10% FBS. The materials degrade faster in the simulated fluid because it doesn’t contain amino acids which may have helped supplement the gelatin nanofiber scaffold and which may have contributed to the maintenance of its structural integrity.

Morphology of cross-linked scaffolds in different media was also studied. Regardless of cross-linker concentration and medium type, gelatin nanofibers completely fused into an undefined mesh after incubation. SEM images of sIPN NS2X, 4X, and 8X samples after 24-h incubation in SSF are presented in Figure 6. One possible postulation is hydrophilic gelatin interacts directly with the surrounding solution, allowing water molecules to penetrate the porous gelatin network and causing fiber expansion and fusion within the scaffold.

3.5. Mucin absorption and cell attachment

Mucin absorption can be used to measure material mucoadhesiveness because it is a critical protein surrounding the oral mucosa epithelial layer [28]. The mucus, from which mucin is derived, plays a role in bioadhesion of [29]. In the oral mucosa, mucus is secreted by the major and minor salivary glands as part of saliva [30, 31]. At physiological pH, the mucus network can form a strongly cohesive gel structure that binds to the epithelial cell surface as a gelatinous layer on the oral mucosa [32].

PEG is well known as a nonfouling polymer. Therefore, it was expected to see low or no mucin absorption on the PEG-only HS. However, PEG-only HS exhibited a slightly negative mucin absorption value as reported in Figure 7. This was presumably due to swelling of the scaffold, which slightly concentrated the mucin solution as a result of solution volume reduction. As for cross-linked gelatin scaffolds, mucin absorption measurement can be influenced by multiple factors including stability, porosity, swelling, and PEG composition of the scaffold. Release of gelatin in to the medium was still likely due to instability of the scaffold although the scaffold was immersed in mucin solution and taken out immediately. Because Bradford protein assay measures protein concentrations non-specifically, we reported mucin absorption in terms of apparent surface density to make it distinct from actual mucin absorption. Among all the tested cross-linked gelatin scaffolds, only sIPN NS4X shows a positive mucin absorption value. Its apparent mucin surface density is 0.2 mg/cm^2. This net positive mucin absorption on sIPN NS4X was achieved because of it well-balanced structure, composition, and properties: it is more stable than sIPN NS2X, has less PEG content than sIPN NS8X, and is more porous than sIPN HS4X. Since only sIPN NS4X promoted mucin absorption and was relatively stable, we further tested fibroblast cell attachment on this scaffold.

Fibroblasts are adherent cells and are a critical component of the oral mucosa because of their ability to proliferate and produce the extracellular matrix of the lamina propria layer [33]. As shown in Figure 8, adherent fibroblasts still stay on the scaffold after 48-h culture. However, there were about 7500 adherent viable fibroblasts found on the sIPN NS4X scaffold, which was 73% less than the cells on TCPS. This low number of adherent cells could be the net result of comprised cell attachment, growth, and proliferation on the scaffold. In addition, those cells penetrated into the scaffold were not included in the count, which could cause an underestimation of the adherent cells.

3.6. In vitro drug release

sIPN NS2X, 4X and 8X scaffolds-loaded with nystatin were used in the drug release study due to their good stability in aqueous conditions. Nystatin was released from sIPN NS2X and 4X scaffolds faster than from sIPN NS8X. Nearly 100% release was completed in 120 h (Figure 9). In contrast, sIPN NS8X released 36.3% of loaded drug within the same period of time. The low mass loss and low swelling of sIPN NS8X contributed to a much slower release than sIPN NS2X and 4X. Given the fact that the maximal duration of buccal drug delivery is 4–6 h due to meal intake and/or drinking[34], further studies are required to manipulate sIPN NS-based formulations to achieve a higher percentage cumulative release in 6 h.

4. Conclusions

In this work, we fabricated electrospun gelatin nanofibers and cross-linked them with PEG-DA575 to form sIPN nanofiber scaffolds. Cross-linking gelatin nanofibers with PEG-DA575 satisfactorily maintained nanofiber structure and morphology. Serial structural parameters and properties of the resulting sIPN scaffolds can be modulated by changing cross-linker concentration. Moreover, PEG-DA was successful in enhancing the structural stability of the

scaffold in aqueous solutions. Through this preliminary investigation, we identified sIPN NS4X as a scaffold that be further studied in the future work. The influence of PEG-DA length on sIPN scaffolds' properties will be evaluated in future studies. Cell viability studies will be performed over time to determine how access to the sIPN can be further improved. The mucin absorption studies suggest that sIPN NS4X scaffolds will likely encourage greater mucoadhesion. Nonetheless, more direct and rigorous testing will be conducted in the future to evaluate this scaffold on *in vitro and ex vivo* oral mucosa tissues. Additionally, compatibility, *in vitro* and *in vivo* anti-fungal activity of nystatin-loaded sIPN gelatin nanofiber scaffolds will be examined.

Acknowledgments

This work was supported, in part, by the National Science Foundation CAREER award (CBET0954957). D. C. A. thanks SREB-State Doctoral Scholars Program. Scanning electron microscopy was performed at the VCU-Dept. of Neurobiology & Anatomy Microscopy Facility, supported with funding from NIH-NINDS Center core grant 5P30NS047463 and NIH-NCRR grant 1S10RR022495.

References

1. Sankar V, Hearnden V, Hull K, Juras DV, Greenberg MS, Kerr AR, et al. Local drug delivery for oral mucosal diseases: challenges and opportunities. Oral Dis. 2011; 17 (Suppl 1):73–84. [PubMed: 21382140]
2. Shojaei AH. Buccal mucosa as a route for systemic drug delivery: a review. J Pharm Pharm Sci. 1998; 1:15–30. [PubMed: 10942969]
3. de Vries ME, Bodde HE, Verhoef JC, Junginger HE. Developments in buccal drug delivery. Crit Rev Ther Drug Carrier Syst. 1991; 8:271–303. [PubMed: 1954653]
4. Hearnden V, Sankar V, Hull K, Juras DV, Greenberg M, Kerr AR, et al. New developments and opportunities in oral mucosal drug delivery for local and systemic disease. Adv Drug Deliv Rev. 2012; 64:16–28. [PubMed: 21371513]
5. Sudhakar Y, Kuotsu K, Bandyopadhyay AK. Buccal bioadhesive drug delivery--a promising option for orally less efficient drugs. J Control Release. 2006; 114:15–40. [PubMed: 16828915]
6. de Araujo DR, Padula C, Cereda CM, Tofoli GR, Brito RB Jr, de Paula E, et al. Bioadhesive films containing benzocaine: correlation between in vitro permeation and in vivo local anesthetic effect. Pharm Res. 2010; 27:1677–86. [PubMed: 20422264]
7. Remunan-Lopez C, Portero A, Vila-Jato JL, Alonso MJ. Design and evaluation of chitosan/ethylcellulose mucoadhesive bilayered devices for buccal drug delivery. J Control Release. 1998; 55:143–52. [PubMed: 9795035]
8. Epstein JB, Truelove EL, Izutzu KT. Oral candidiasis: pathogenesis and host defense. Rev Infect Dis. 1984; 6:96–106. [PubMed: 6369482]
9. Samaranayake LP, Keung Leung W, Jin L. Oral mucosal fungal infections. Periodontology 2000. 2009; 49:39–59. [PubMed: 19152525]
10. Matthews JA, Wnek GE, Simpson DG, Bowlin GL. Electrospinning of collagen nanofibers. Biomacromolecules. 2002; 3:232–8. [PubMed: 11888306]
11. Boland ED, Matthews JA, Pawlowski KJ, Simpson DG, Wnek GE, Bowlin GL. Electrospinning collagen and elastin: preliminary vascular tissue engineering. Front Biosci. 2004; 9:1422–32. [PubMed: 14977557]
12. Barnes CP, Pemble CW, Brand DD, Simpson DG, Bowlin GL. Cross-linking electrospun type II collagen tissue engineering scaffolds with carbodiimide in ethanol. Tissue Eng. 2007; 13:1593–605. [PubMed: 17523878]
13. Zhang Z, Hu J, Ma PX. Nanofiber-based delivery of bioactive agents and stem cells to bone sites. Adv Drug Deliv Rev. 2012; 64:1129–41. [PubMed: 22579758]
14. Hu J, Ma PX. Nano-fibrous tissue engineering scaffolds capable of growth factor delivery. Pharm Res. 2011; 28:1273–81. [PubMed: 21234657]

15. Wei G, Ma PX. Nanostructured Biomaterials for Regeneration. Adv Funct Mater. 2008; 18:3566–82. [PubMed: 19946357]
16. Sill TJ, von Recum HA. Electrospinning: applications in drug delivery and tissue engineering. Biomaterials. 2008; 29:1989–2006. [PubMed: 18281090]
17. Barnes CP, Sell SA, Boland ED, Simpson DG, Bowlin GL. Nanofiber technology: designing the next generation of tissue engineering scaffolds. Adv Drug Deliv Rev. 2007; 59:1413–33. [PubMed: 17916396]
18. Burmania JA, Martinez-Diaz GJ, Kao WJ. Synthesis and physicochemical analysis of interpenetrating networks containing modified gelatin and poly(ethylene glycol) diacrylate. J Biomed Mater Res A. 2003; 67:224–34. [PubMed: 14517880]
19. Fu Y, Kao WJ. Drug release kinetics and transport mechanisms from semi-interpenetrating networks of gelatin and poly(ethylene glycol) diacrylate. Pharm Res. 2009; 26:2115–24. [PubMed: 19554430]
20. Milleret V, Simona B, Neuenschwander P, Hall H. Tuning electrospinning parameters for production of 3D-fiber-fleeces with increased porosity for soft tissue engineering applications. Eur Cell Mater. 2011; 21:286–303. [PubMed: 21432783]
21. Sell SA, Francis MP, Garg K, McClure MJ, Simpson DG, Bowlin GL. Cross-linking methods of electrospun fibrinogen scaffolds for tissue engineering applications. Biomed Mater. 2008; 3:045001. [PubMed: 18824779]
22. Hu YH, Grainger DW, Winn SR, Hollinger JO. Fabrication of poly(alpha-hydroxy acid) foam scaffolds using multiple solvent systems. J Biomed Mater Res. 2002; 59:563–72. [PubMed: 11774315]
23. Ritschel WA, Tompson GA. Monitoring of drug concentrations in saliva: a non-invasive pharmacokinetic procedure. Methods Find Exp Clin Pharmacol. 1983; 5:511–25. [PubMed: 6363838]
24. Groll AH, Mickiene D, Werner K, Piscitelli SC, Walsh TJ. High-performance liquid chromatographic determination of liposomal nystatin in plasma and tissues for pharmacokinetic and tissue distribution studies. J Chromatogr B Biomed Sci Appl. 1999; 735:51–62. [PubMed: 10630890]
25. Sell S, Barnes C, Simpson D, Bowlin G. Scaffold permeability as a means to determine fiber diameter and pore size of electrospun fibrinogen. Journal of Biomedical Materials Research, Part A. 2008; 85A:115–26. [PubMed: 17688269]
26. Liu X, Ma PX. Phase separation, pore structure, and properties of nanofibrous gelatin scaffolds. Biomaterials. 2009; 30:4094–103. [PubMed: 19481080]
27. Zhang Y, Ouyang H, Lim CT, Ramakrishna S, Huang ZM. Electrospinning of gelatin fibers and gelatin/PCL composite fibrous scaffolds. J Biomed Mater Res B Appl Biomater. 2005; 72:156–65. [PubMed: 15389493]
28. Takeuchi H, Thongborisute J, Matsui Y, Sugihara H, Yamamoto H, Kawashima Y. Novel mucoadhesion tests for polymers and polymer-coated particles to design optimal mucoadhesive drug delivery systems. Adv Drug Deliv Rev. 2005; 57:1583–94. [PubMed: 16169120]
29. Peppas NA, Buri PA. Surface, interfacial and molecular aspects of polymer bioadhesion on soft tissues. J Controlled Release. 1985; 2:257–75.
30. Tabak LA, Levine MJ, Mandel ID, Ellison SA. Role of salivary mucins in the protection of the oral cavity. J Oral Pathol. 1982; 11:1–17. [PubMed: 6801238]
31. Rathbone MJ, Drummond BK, Tucker IG. The Oral Cavity as a Site for Systemic Drug-Delivery. Adv Drug Deliver Rev. 1994; 13:1–22.
32. Gandhi RB, Robinson JR. Oral cavity as a site for bioadhesive drug delivery. Adv Drug Deliver Rev. 1994; 13:43–74.
33. Kinikoglu B, Rodriguez-Cabello JC, Damour O, Hasirci V. The influence of elastin-like recombinant polymer on the self-renewing potential of a 3D tissue equivalent derived from human lamina propria fibroblasts and oral epithelial cells. Biomaterials. 2011; 32:5756–64. [PubMed: 21592566]
34. Khanvilkar K, Donovan MD, Flanagan DR. Drug transfer through mucus. Adv Drug Delivery Rev. 2001; 48:173–93.

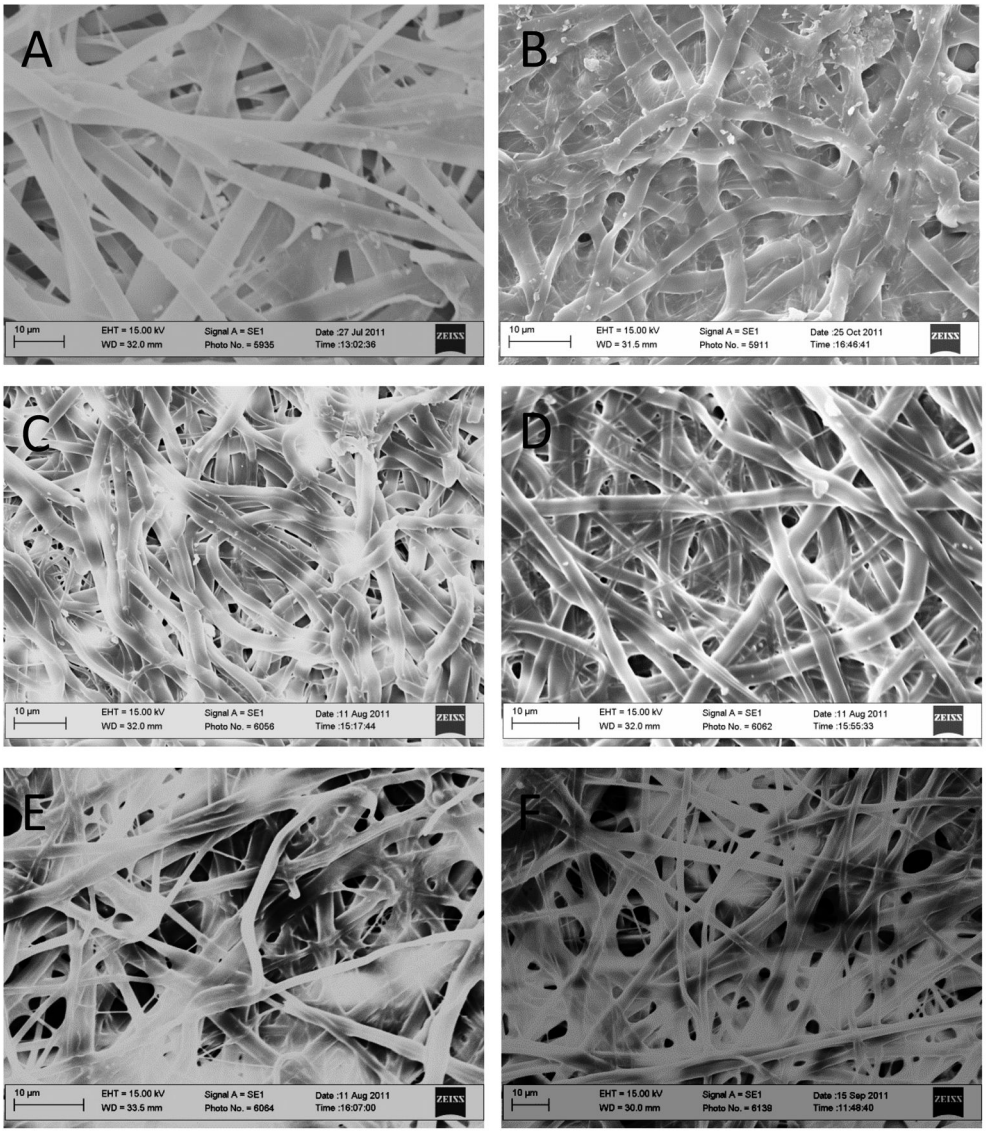

Figure 1.
SEM image of gelatin NS(A), NSE (B), sIPN NS1X (C), sIPN NS2X (D), sIPN NS4X (E), and sIPN NS8X (F). Bars: 10 μm.

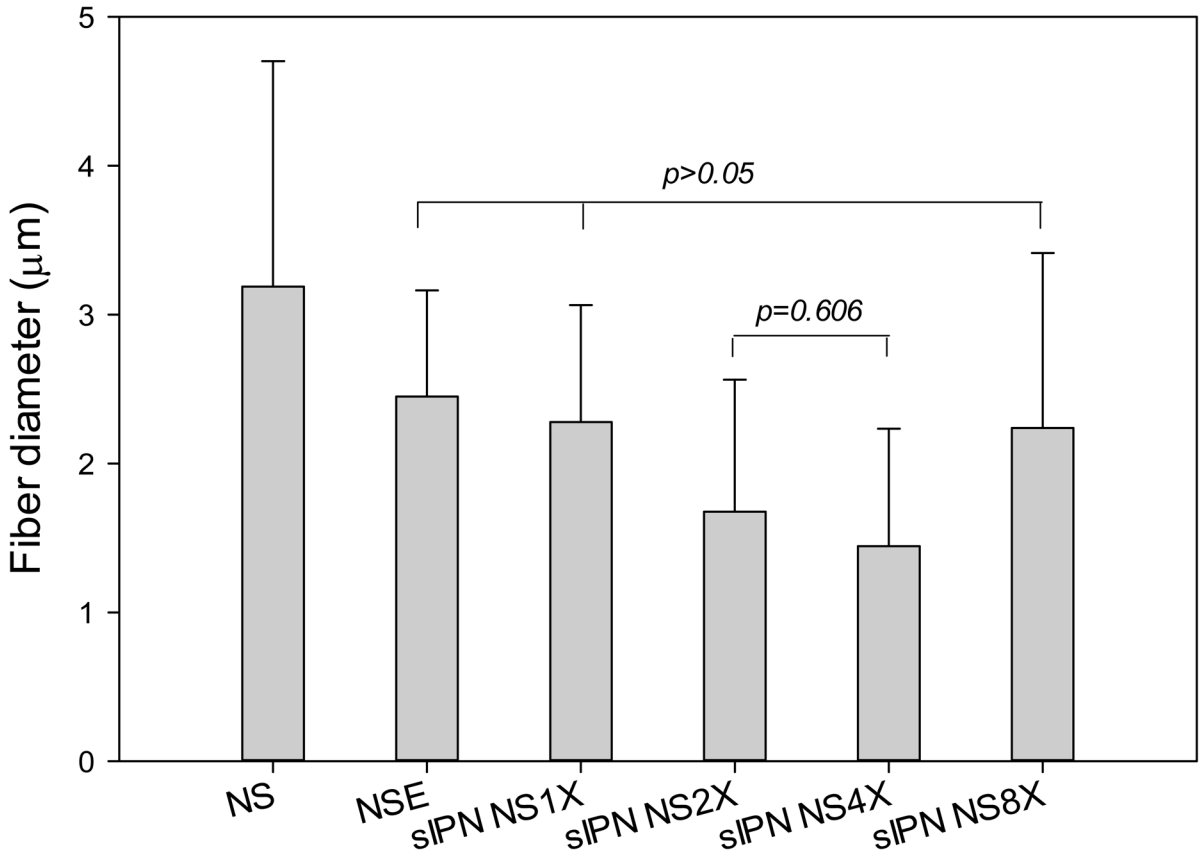

Figure 2.
Fiber diameters of electrospun gelatin nanofibers (n=62) receiving different treatments. Analysis of one way ANOVA followed by Holm-Sidak method showed that a statistically significant difference ($p<0.05$) existed between any two subgroups unless noted above (p=0.577 for NSE *vs.* sIPN NS1X, p=0.578 for NSE *vs.* sIPN NS8X, and p=0.830 for sIPN NS1X *vs.* sIPN NS8X).

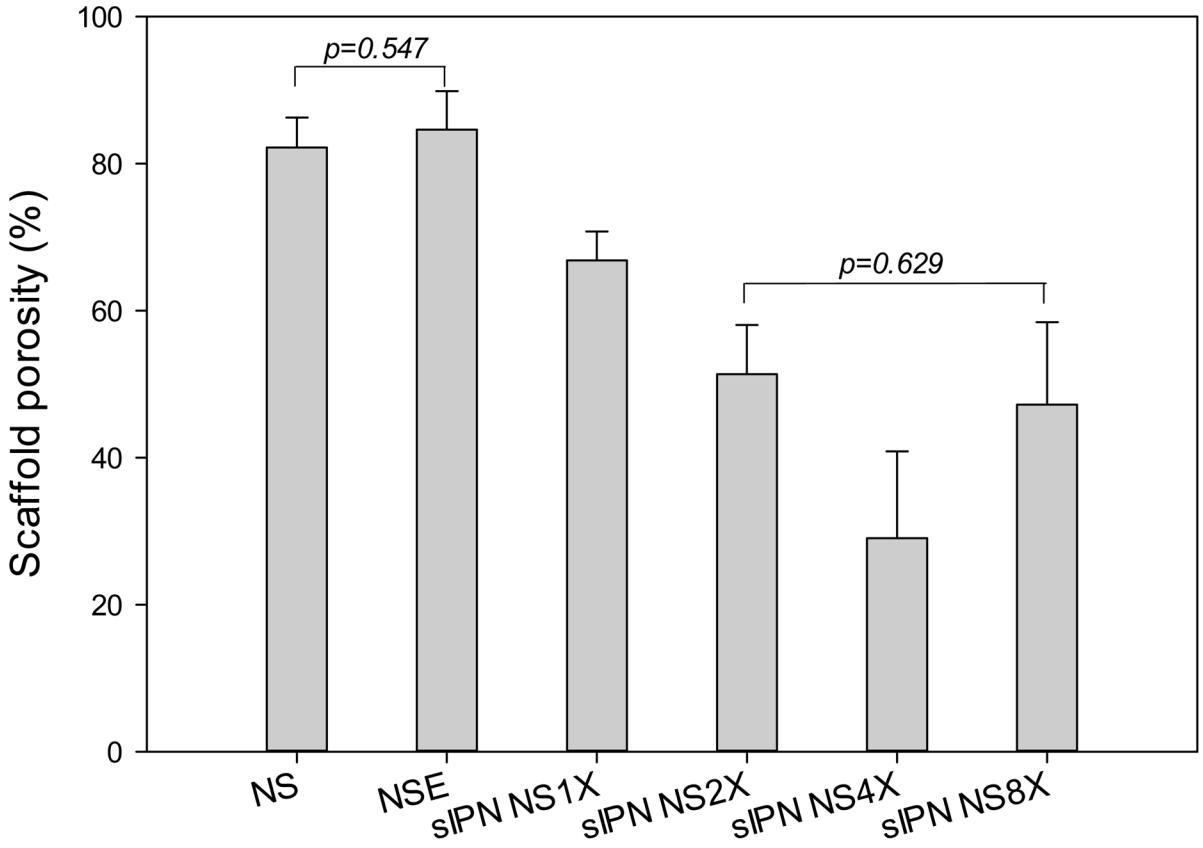

Figure 3.
Porosity of electrospun gelatin nanofiber scaffolds receiving different treatments (n=5). One way ANOVA followed by Holm-Sidak method for all pairwise multiple comparison of any two subgroups indicate that there is a statistically significant difference between any two subgroups except for NS *vs.* NSE, and sIPN NS2X *vs.* sIPN NS8X.

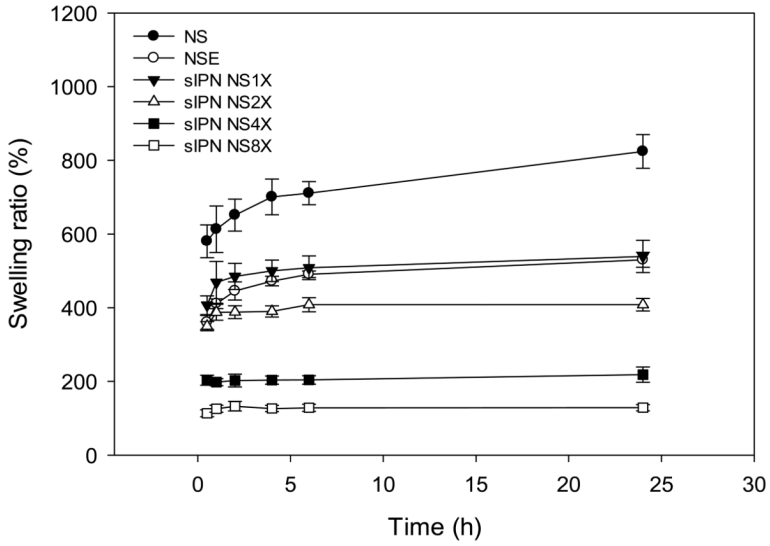

Figure 4.
Swelling kinetics of electrospun gelatin nanofiber scaffolds receiving different treatments in pH 7.4 PBS at room temperature (24 °C).

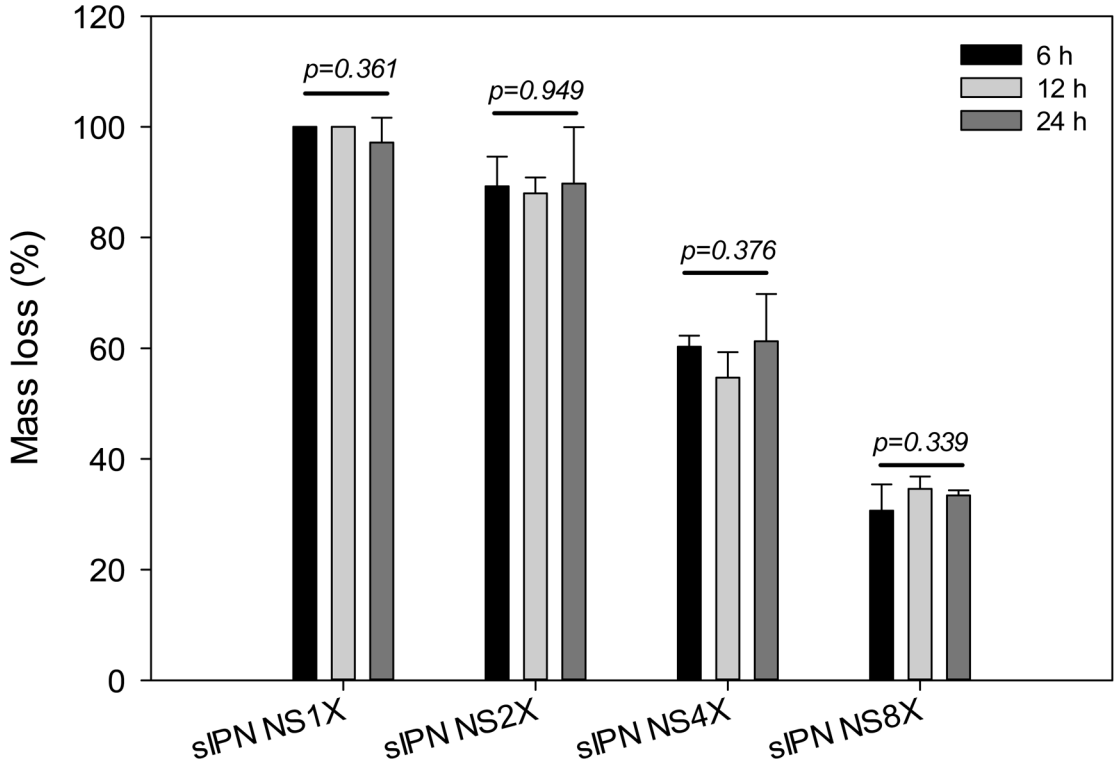

Figure 5A

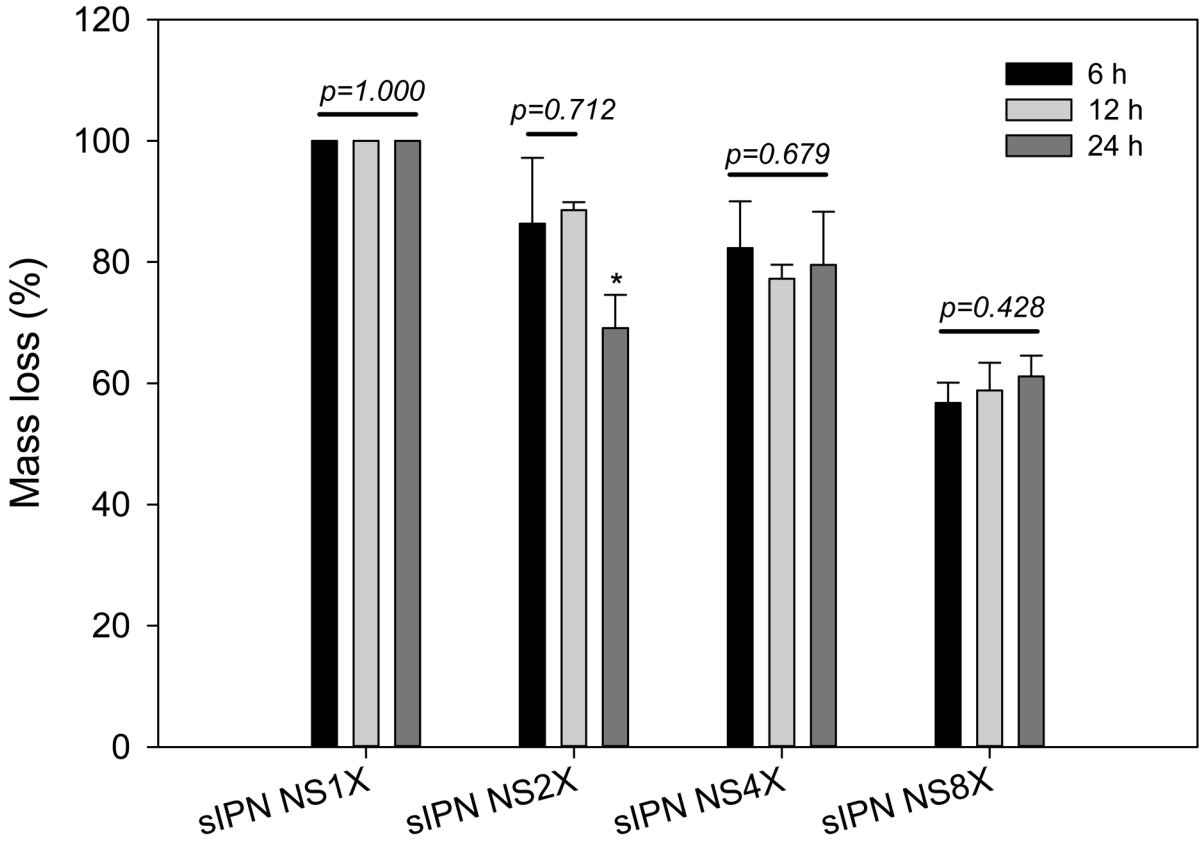

Figure 5B

Figure 5.
In vitro degradation of sIPN NS1X, 2X, 4X, and 8X (n=3) in DMEM/10% FBS (A), and SSF (B) for various lengths of incubation (6, 12, and 24 h). * indicates a significant difference from either 6h or 12h.

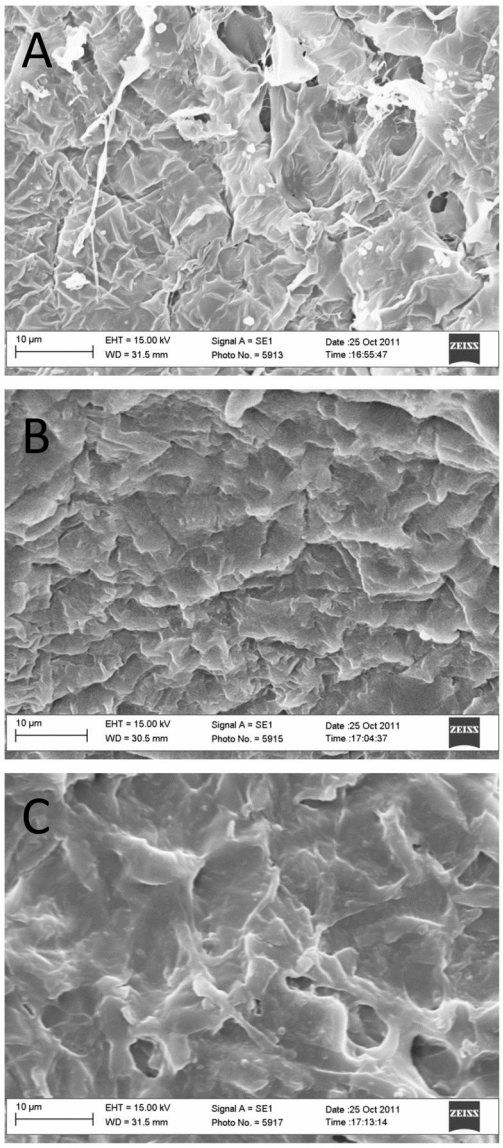

Figure 6.
SEM images of cross-linked scaffolds (A: sIPN NS2X, B: sIPN NS4X, and C: sIPN NS8X) following 24h-incubation in SSF. SEM images of NS, NSE, and sIPN NS1X were not taken due to their complete mass loss during incubation.

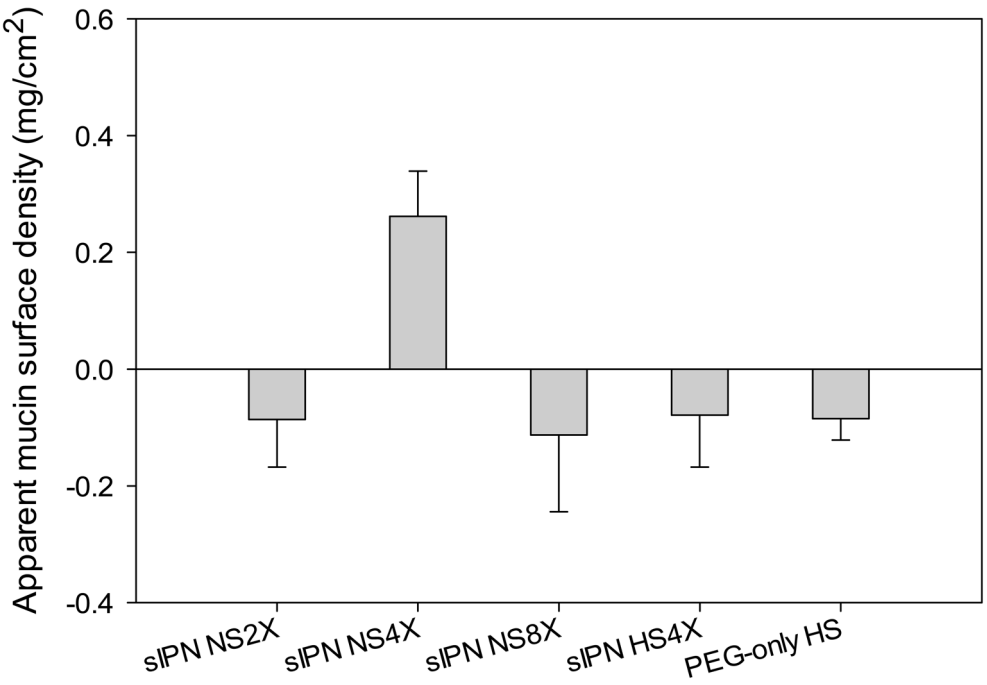

Figure 7.
Apparent mucin density on the surface of scaffolds including sIPN NS2X, 4X, 8X, sIPN HS4X, and PEG-only HS.

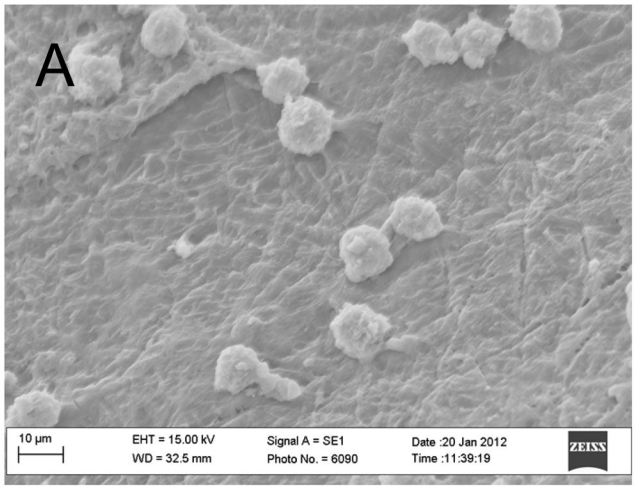

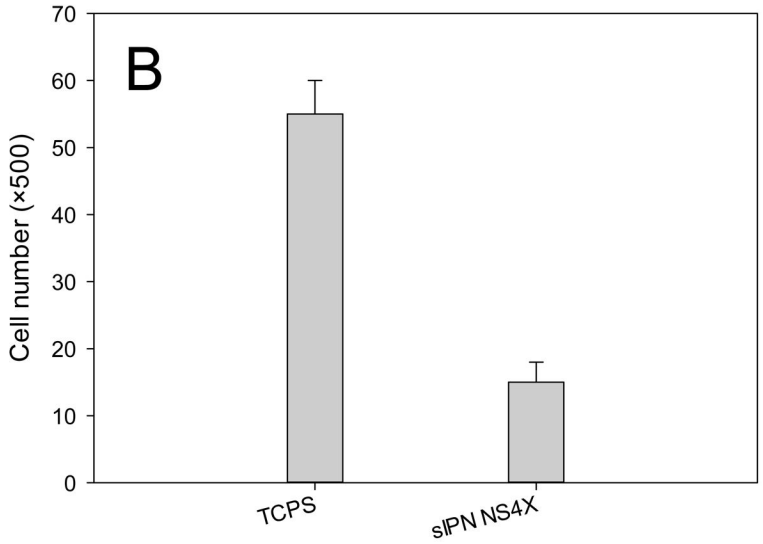

Figure 8.
Cell attachment on sIPN NS4X. (A) SEM image of adherent human dermal fibroblasts on sIPN NS4X following 48-h culture; (B) Quantification of adherent cells on TCPS (control) and sIPN NS4X with trypan blue assay.

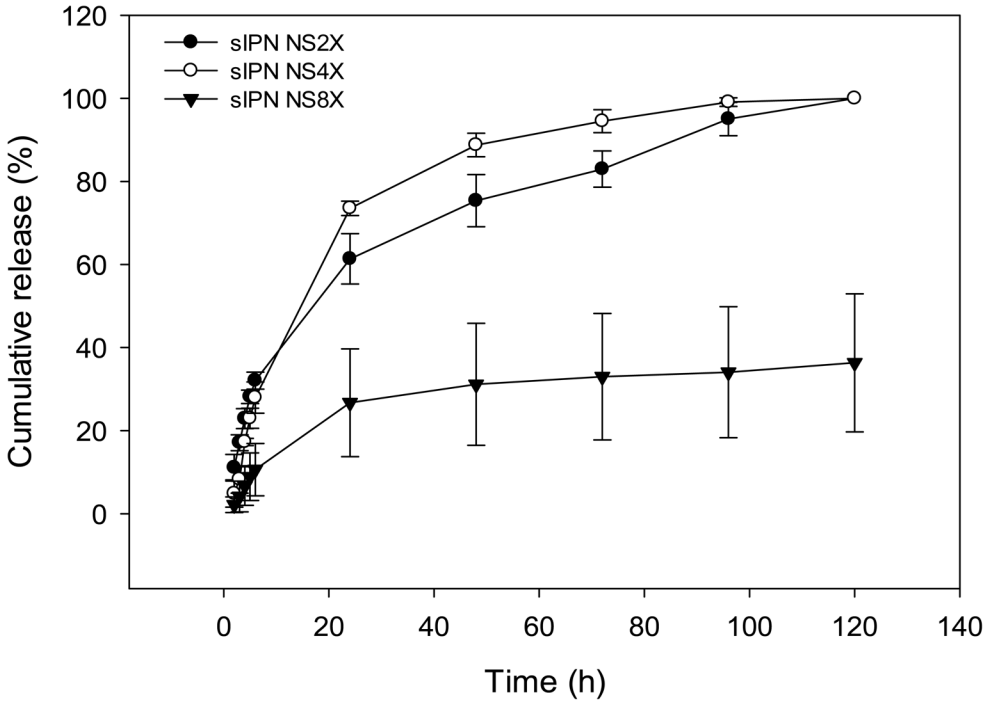

Figure 9.
Cumulative release of nystatin from sIPN NS2X, 4X, and 8X in pH 7.4 PBS at 37 °C.

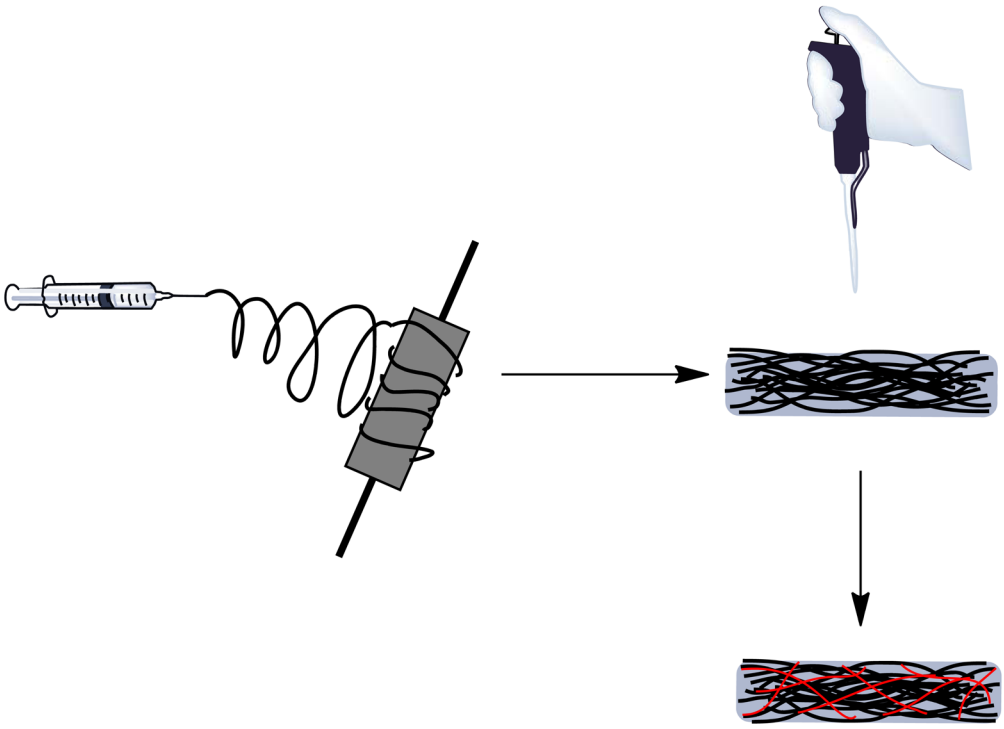

Scheme 1.

Preparation of sIPN NS by a two-step process. Step 1: electrospinning of gelatin or a mixture of gelatin and nystatin to obtain a nanofiber scaffold (NS); Step 2: The resulting NS was incubated with various concentrations of PEG-DA575 along with DMPA in ethanol for 30 min, subjected to UV light for 2 min on each side of the scaffold, and air-dried to obtain sIPN NS.

Table 1

Mechanical properties of the fabricated gelatin nanofiber scaffolds

Sample	Thickness (in)	Peak load (N)	Peak stress (MPa)	Modulus (MPa)	Strain at break (mm/mm)	Energy to break (N×mm)
NS	0.00915 ± 0.0012	1.062 ± 0.5374	1.759 ± 1.004	94.3 ± 41.4	0.0286 ± 0.0120	0.1045 ± 0.0762
NSE	0.0130 ± 0.0067	16.04± 6.791	18.36± 9.266	606.5± 201.9	0.0460± 0.0134	3.199±1.989
sIPN NS1X	0.0200 ± 0.0027	22.07 ± 5.416	17.48 ± 4.758	554.5 ± 153.8	0.0580 ± 0.0180	5.758 ± 1.842
sIPN NS2X	0.0220 ± 0.0104	16.61 ± 5.285	12.40 ± 5.126	383.8 ± 196.7	0.0520 ± 0.0094	3.775 ± 2.029
sIPN NS4X	0.0220 ± 0.0043	12.44 ± 1.922	8.715 ± 1.440	251.0 ± 53.6	0.0700 ± 0.0166	4.242 ± 1.111
sIPN NS8X	0.0300 ± 0.0029	13.50 ± 1.846	6.609 ± 1.080	155.5 ± 30.4	0.0950 ± 0.023	5.941± 1.928